Malaysian Journal of Chemistry, 2025, Vol. 27(2), 148-158

Development of a Biocompatible Blend Electrolyte System of Epoxidized Natural Rubber (ENR-25 and ENR-50)/ Chitosan (CTS)/ Lithium Perchlorate ($LiClO_4$)

Shazlynn Alia Saiful Sharmizam[1], Hussein Hanibah[2]*, Nor Zakiah Nor Hashim[2], Belinda Jane Agong[1], Nur Syazwani Rahmie Rahman[1] and Azizan Ahmad[3]
[1]Faculty of Applied Sciences, Universiti Teknologi MARA, Shah Alam, 40450 Shah Alam, Selangor, Malaysia
[2]Centre of Foundation Studies, Universiti Teknologi MARA, Cawangan Selangor, Kampus Dengkil, 43800 Dengkil, Selangor, Malaysia.
[3]Polymer Research Center, Faculty of Science and Technology, Universiti Kebangsaan Malaysia, 43600 Bangi, Selangor, Malaysia
*Corresponding author (e-mail: drhussein@uitm.edu.my)

Polymer blend electrolytes (PBE) are efficient electrolyte systems that hold great potential in various applications, especially fuel cells and lithium-ion batteries. Their ongoing development has the potential to advance energy storage technology, resulting in better and longer-lasting capacity degradation. For this study, a solvent casting method was used to mix epoxidized natural rubber (ENR), chitosan (CTS) and lithium perchlorate ($LiClO_4$), while maintaining the 50:50 polymer ratio for each level of ENR. The mix of ENR grades and CTS had different levels of miscibility, which was supported by ATR-FTIR analysis of the chemical structure and the changes that happened when $LiClO_4$ was added. For each blend, TGA analysis identified two stages of thermal degradation that occurred at various temperatures. In the case of the ENR-25/CTS blend, these stages were observed at 231 °C and 345 °C, while for the ENR-50/CTS blend, they occurred at 233-343 °C with T_{max} at 250 °C and 343-482 °C with T_{max} at 378 °C, respectively. The ATR-FTIR analysis showed that the Li^+ cations in the ENR/CTS/$LiClO_4$ blend electrolyte samples interacted with the NH_2 and C-O-C groups. Impedance analysis revealed conductivity values of 2.58×10^{-3} S/cm for the ENR-25/CTS/$LiClO_4$ blend, and 3.12×10^{-3} S/cm for the ENR-50/CTS/$LiClO_4$ blend.

Keywords: Epoxidized natural rubber; chitosan; polymer blend; lithium perchlorate; conductivity

Received: March 2024; Accepted: February 2025

Polymer electrolyte systems have gained significant attention over the past few decades for their potential use in various applications, such as fuel cells, batteries and supercapacitors [1]. Researchers have been exploring the use of polymer blends as an electrolyte material to improve ionic conductivity, biocompatibility, and stability, mainly in battery applications [2]. However, most battery systems still consist of synthetic materials that harm the environment [3]. One potentially effective approach to addressing environmental issues associated with traditional battery technology is the utilisation of biodegradable materials and inorganic salts in biodegradable rechargeable battery systems. Biodegradable materials can naturally decompose over time through biological processes, which reduces the environmental impact associated with battery disposal and waste management [4].

Epoxidized natural rubber (ENR) is a natural rubber (NR) that incorporates epoxy groups in its backbone chain, as shown in Figure 1. Jantanasakulwong et al. (2016) stated that ENR has different epoxidation levels; however, the most commonly used are ENR-75, ENR-50, and ENR-25 [5]. Abu Bakar et al. (2008) mentioned that ENR is used in diverse applications, such as the synthesis and modification of polymers and polymer blends [6]. Typically, ENR is made by changing NR chains chemically in a simple way using acid and hydrogen peroxide (H_2O_2) to react with an oxygen atom that has double bonds. However, its high gel content, low ionic conductivity, high molecular weight, and poor chemical and physical properties are drawbacks to its solubility and processability [7]. As explained by Stephens et al. (2001), physical or chemical changes should be carried out to improve these substantial limitations. Examples of modifications include chemical bonding between the rubber chains and other polymers, or free-radical grafting conducted on ENR. Free-radical grafting on ENR may have an impact on the physical and chemical properties of the polymer material.

The linear polysaccharide that consists of D-glucosamine and N-acetyl-D-glucosamine is known as chitosan (CTS) and has higher mechanical ability, biodegradability, compatibility, antibacterial activity, high ionic conductivity, and non-toxicity [8]. CTS carries amine (NH_2) groups, which can interact easily with other reactive groups. Ionic interactions, graft reactions, and chemical alteration have changed the structure of CTS. There has been significant development in the modification of CTS and the use of its derivatives, including a variety of reactions, condition optimisation, and new synthetic pathways. Since modified CTS often has better chemical characteristics than unmodified CTS, CTS derivatives have been widely used and have more promising prospects. N-carboxymethyl chitosan (CMC), chitosan oligosaccharides (COS), quaternized chitosan (QCS), CTS nanoparticles, and CTS-based hydrogels are a few examples of the diverse range of CTS derivatives [9]. CTS is hydrophilic and soluble in water and acids at a pH of 6.5. CTS has a variety of uses because of its physical and chemical properties, especially in the pharmaceutical, clothing, food, agricultural, biomedical, and cosmetics industries [5].

The selection of epoxidized natural rubber (ENR) and chitosan (CTS) as polymer blend components was driven by their complementary properties, which make them particularly suitable for polymer blend electrolytes. ENR was chosen for its flexibility, chemical stability, and ability to interact with lithium salts, which enhances ionic conductivity. Its elastomeric nature allows for improved mechanical strength and flexibility in the polymer matrix, which is crucial for applications that require durable, yet conductive, materials [10, 11]. Chitosan is a biopolymer known for its excellent film-forming properties, biocompatibility, and ability to form complexes with lithium ions. It provides mechanical stability while also facilitating ionic conduction through its interactions with the lithium salt. Moreover, CTS contributes to the environmental friendliness and sustainability of the material, as it is derived from natural sources. These specific polymers offer a balance of mechanical flexibility (from ENR) and structural reinforcement (from CTS) that is often not achievable with other polymer systems [11-12]. Compared to other synthetic polymers, ENR and CTS provide an ideal combination of biocompatibility, mechanical integrity, and ionic conductivity, making them highly suitable for applications in solid polymer electrolytes.

Characterization methods such as Fourier transform infrared spectroscopy (FTIR), electrochemical impedance spectroscopy (EIS), and thermogravimetric analysis (TGA) can be used to perform polymer characterization. In this study, different epoxidation levels of ENR were mixed with CTS. According to Taweepreda et al. (2014), it's due to the good interfacial contacts and the way CTS interacts with the backbone of ENR-25 during polymer blend by using a casting method [13]. Lithium perchlorate ($LiClO_4$) is often used in polymer electrolytes as it breaks down into lithium cations and perchlorate anions, making it easier for ions to move through the electrolyte. Its high ionic conductivity, coupled with its good solubility in various polymer matrices, including ENRs and CTS, further enhances the performance of the electrolyte [14]. The use of $LiClO_4$ enhances the ionic conductivity of the electrolyte system, leading to better electrochemical reactions and overall battery performance. The improved ionic conductivity results in an enhanced power output, faster charging or discharging rates, and increased energy efficiency in the battery system [15-16].

However, the full potential of a blended electrolyte system remains to be explored [17]. This study aims to comprehensively understand the properties and potential of ENR-25/CTS and ENR-50/CTS blended electrolyte systems with a 50:50 ratio. The synthesis and characterization of the blend will provide valuable information on its chemical composition, thermal stability, and ionic conductivity at different ENRs and CTS ratios.

We started with the 50:50 ratio for ENR and CTS based on preliminary optimization, which indicated that this composition offered an optimal balance between the mechanical flexibility provided by ENR and the structural reinforcement and ionic interaction capacity of CTS. This ratio also agreed with findings from previous studies on polymer blend electrolytes, which indicate that a balanced composition often leads to improved performance in terms of ionic conductivity and thermal stability.

By doping $LiClO_4$ at various ratios, the optimum conductivity value can be determined, leading to insights on improving the conductivity of the blended system. The development of an optimized blended system with improved biocompatibility, stability, and conductivity compared to existing electrolyte systems would be a significant contribution to the field of energy storage [18-19].

By addressing the environmental concerns associated with battery waste and reducing the reliance on non-renewable materials, this research contributes to the progress of green energy technologies. Implementation of a biodegradable blended electrolyte system in secondary batteries has the potential to revolutionise the energy storage landscape and pave the way towards a more sustainable and eco-friendly future.

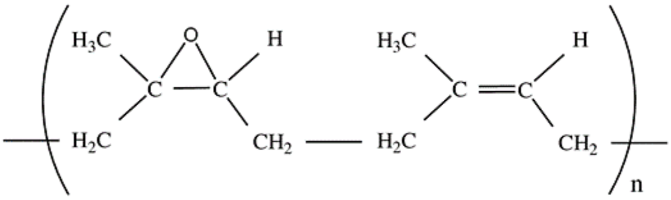

Figure 1. The chemical structure of epoxidized natural rubber (ENR)[20].

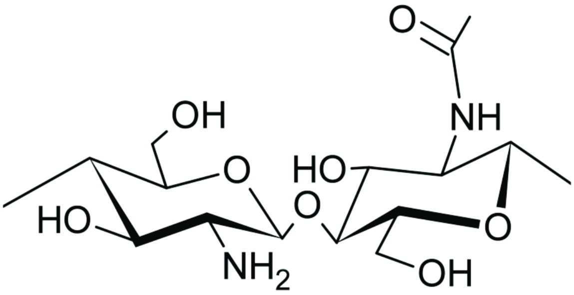

Figure 2. The chemical structure of chitosan (CTS)[21].

EXPERIMENTAL

Chemicals and Materials

Epoxidized natural rubber (ENR) with 25 % and 50 % epoxidation levels were obtained from Lembaga Getah Malaysia. Chitosan (CTS) was purchased from Xi'an Lanshan Biotechnology Co., Ltd, China. Acetic acid 99.8 % (CH_3COOH), lithium perchlorate 99.9 % ($LiClO_4$), tetrahydrofuran (THF), toluene, *n*-hexane and methanol were purchased from Biomics Solution Sdn Bhd, Malaysia. All solvents used were AR grade.

Purification of ENR

All the ENR was purified using the re-precipitation method. This was accomplished by dissolving the ENR in a non-polar organic solvent and then re-precipitating it in a polar organic solvent. The raw rubber was processed through mastication using a two-roll mill machine, where it was continuously rolled over five times, and the nip gap was reduced from 2 mm to 1 mm. Then, an appropriate amount of ENR was dissolved in analytical grade toluene ($C_6H_5CH_3$) to make a stock solution of 2 % (w/w). This was stirred at 300 revolutions per minute (rpm) using a magnetic stirrer for 48 hours at 70 °C.

The stock solution was filtered using a vacuum pump to extract the soluble ENR from the stock solution, leaving the insoluble part of the ENR at the top of the Büchner funnel (the gel content). The soluble ENR was left to dry overnight in the fume hood to allow any remaining solvent to evaporate naturally, producing a very viscous solution.

This viscous solution was poured with continuous stirring into methanol at a polymer solution:methanol ratio of 1:5. During the stirring process, a gel-like precipitate of pure ENR was formed. The gel-like ENR was left in the solvent for two hours to complete the re-precipitation process. The precipitate was collected using the rope-trick method with a glass rod and cast onto a Petri dish. This was dried at 50 °C in a conventional oven for 48 hours before being stored in the desiccator.

Purification of CTS

CTS was also purified using a re-precipitation method, by dissolving it in a polar organic solvent and then re-precipitating it in a non-polar organic solvent. An appropriate amount of CTS was dissolved in acetic acid (CH_3COOH) and deionized water (H_2O) to make a stock solution of 2 % (w/w). This was stirred at a speed of 300 rpm using a magnetic stirrer for 48 hours at 50 °C.

The stock solution was filtered using several layers of cotton gauze and immediately concentrated to less than a third of its initial volume using a rotatory evaporator for 1 hour at 95 °C. In a separating funnel, the concentrated CTS was poured into n-hexane at a polymer solution:n-hexane ratio of 1:5, where it formed a heterogeneous mixture. Later, the organic polymer (bottom layer) was cast onto a Petri dish and dried in a conventional oven for 48 hours at 50 °C before being stored in the desiccator.

Polymer Blending Process of ENR and CTS

The process of blending polymers was synthesized using a solution casting method in a 50:50 ratio of ENR:CTS with continuous stirring.

This was achieved by dissolving the ENR in a non-polar organic solvent and the CTS in a polar solvent, and then combining the two solutions. To produce the ENR/CTS blend, an appropriate amount of purified ENR was dissolved in THF, while purified CTS was dissolved in deionized water (H_2O). The two mixtures were combined in a 50:50 ratio and stirred using a magnetic stirrer for 48 hours at 50 °C until a homogeneous blend was obtained. The blended solution was cast onto a petri dish and dried in a conventional oven for 48 hours at 50 °C before being doped with inorganic salts.

Preparation of ENR/CTS/$LiClO_4$ Blended Electrolyte Film

The preparation of ENR/CTS/$LiClO_4$ blended electrolyte films was carried out using a solution casting method. This was done by doping the ENR/CTS blend with various amounts of lithium perchlorate ($LiClO_4$) ranging from 0 % to 10 %. The blends were stirred with a magnetic stirrer for 24 hours at 50 °C until complete dissolution of the salt was achieved. Each blended electrolyte solution was cast onto a petri dish and left to dry overnight in the fume hood for 72 hours, followed by further drying in a conventional oven for 48 hours at 50 °C, before being stored in the desiccator.

Characterization Methods

Thermogravimetric Analysis (TGA)

Thermogravimetric analysis (TGA) was performed using a TA Q500 instrument. Samples weighing approximately 10–20 mg were placed in a platinum pan and heated under a nitrogen atmosphere at a heating rate of 10 °C min^{-1} over a temperature range of 50–500 °C, respectively.

Fourier Transform Infrared (FTIR)

FTIR spectra were recorded using an attenuated total reflectance (ATR) Bruker Alpha I spectrometer in the range of 4000–650 cm^{-1}, with a resolution of 4 cm^{-1} and 16 scans.

Electrochemical Impedance Spectroscopy (EIS)

The ionic conductivities of the ENR-25/CTS/LiClO4 and ENR-50/CTS/$LiClO_4$ blended electrolyte samples were investigated in order to study the performance of the electrolyte at ambient and elevated temperatures, while maintaining a consistent 50:50 polymer ratio. The impedance spectra were measured using a high-frequency response analyzer (Gamry Potentiostat) with frequencies ranging from 100 Hz to 1 MHz and an amplitude of 100 mV. The ionic conductivity of this blended electrolyte was calculated using Equation 1 below:

$$\sigma = \frac{1}{R}\left(\frac{L}{A}\right) \qquad (1)$$

Where:
σ = Conductivity of the material (S/cm)
L = Length of conductor (cm)
R_b = Resistance of the conductor in Ohm (Ω)
A = Cross-section area (cm^2)

RESULTS AND DISCUSSION

Thermogravimetric Analysis (TGA)

The TGA and DTGA curves of the purified CTS, purified ENR-25, and ENR-25/CTS blend are shown in Figure 3, while the TGA and DTGA curves of the purified CTS, purified ENR-50, and ENR-50/CTS blend are presented in Figure 4.

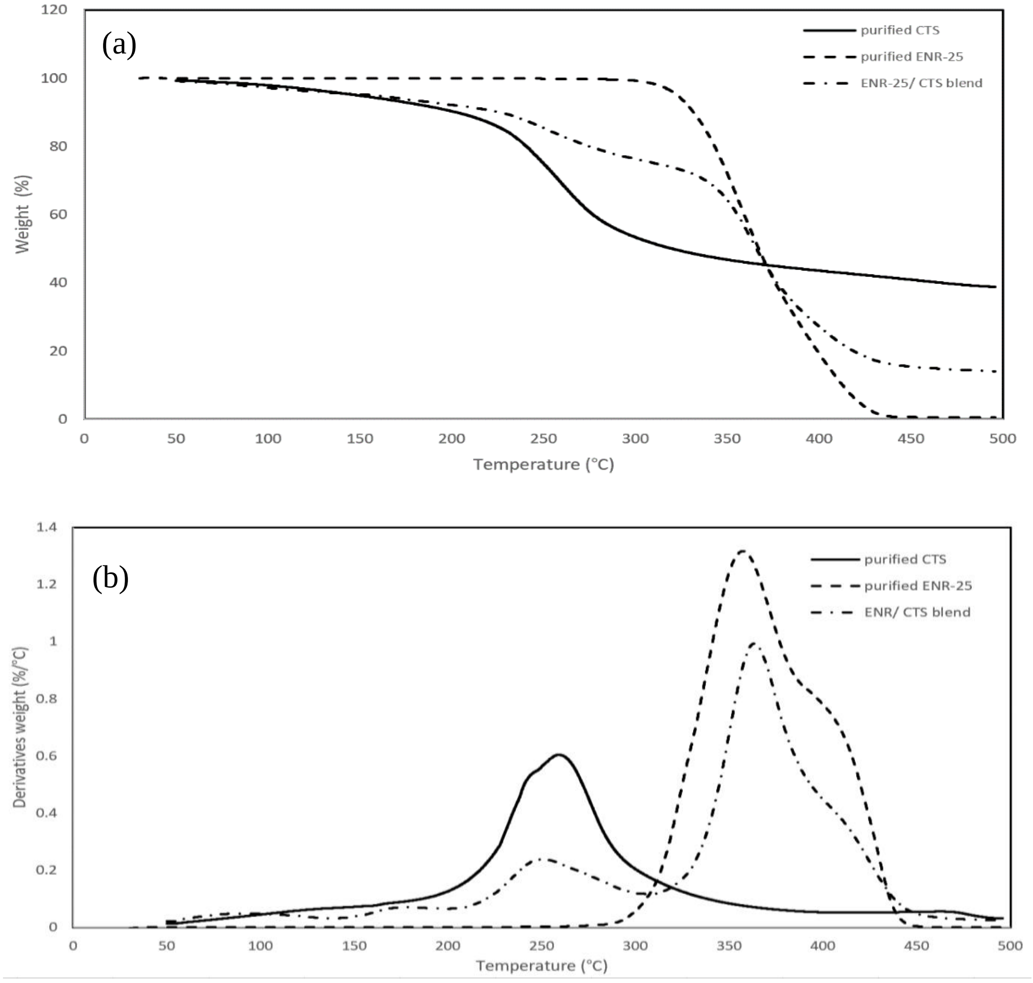

Figure 3. (a) TGA and (b) DTGA curves of the purified CTS, purified ENR-25, and ENR-25/ CTS blend.

The thermal decomposition of purified CTS began at a temperature range of 229–353 °C, with the highest decomposition temperature (T_{max}) occurring at 257 °C, as shown in Figure 3. Riyajan et al. (2013) found that the degradation temperature of CTS fell between 200 and 350 °C [22], which is consistent with our study's results. The purified ENR-25 began to degrade within the temperature range of 328-455 °C, reaching its T_{max} at 356 °C. The ENR-25/CTS blend exhibited two-step decompositions at the temperature ranges of 231-345 °C and 345-480 °C, reaching T_{max} at 251 °C and 362 °C. The initial breakdown stage of the ENR-25/CTS mix involved the elimination of primary chitosan, resulting in a weight loss of around 36 %. The subsequent stage of decomposition involved the elimination of ENR molecules, leading to a weight loss of around 10 %.

Purified ENR-50 began decomposing at 335 °C; this was completed at 473 °C, with a T_{max} of 370 °C. The TGA of the ENR-50/CTS blend differed from that of purified CTS and purified ENR-50, as shown in Figure 4. The polymer blend exhibited two distinct thermal breakdown ranges: one at 233-343 °C with a T_{max} of 250 °C, and another at 343-482 °C with a T_{max} of 378 °C. The initial decomposition stage involved the extraction of primary chitosan resulting in a 20 % weight reduction, whereas the subsequent stage involved the elimination of ENR molecules, leading to a 12 % weight decrease. ENR with 25 % epoxidation levels had greater T_{max} values than ENR with 50 % epoxidation levels, mostly because of the different epoxidation levels. This study focused on overall thermal stability, emphasizing its critical role in understanding material performance. A more detailed investigation into how these factors influence practical applications could provide valuable insights, and addressing this will be a priority in future studies.

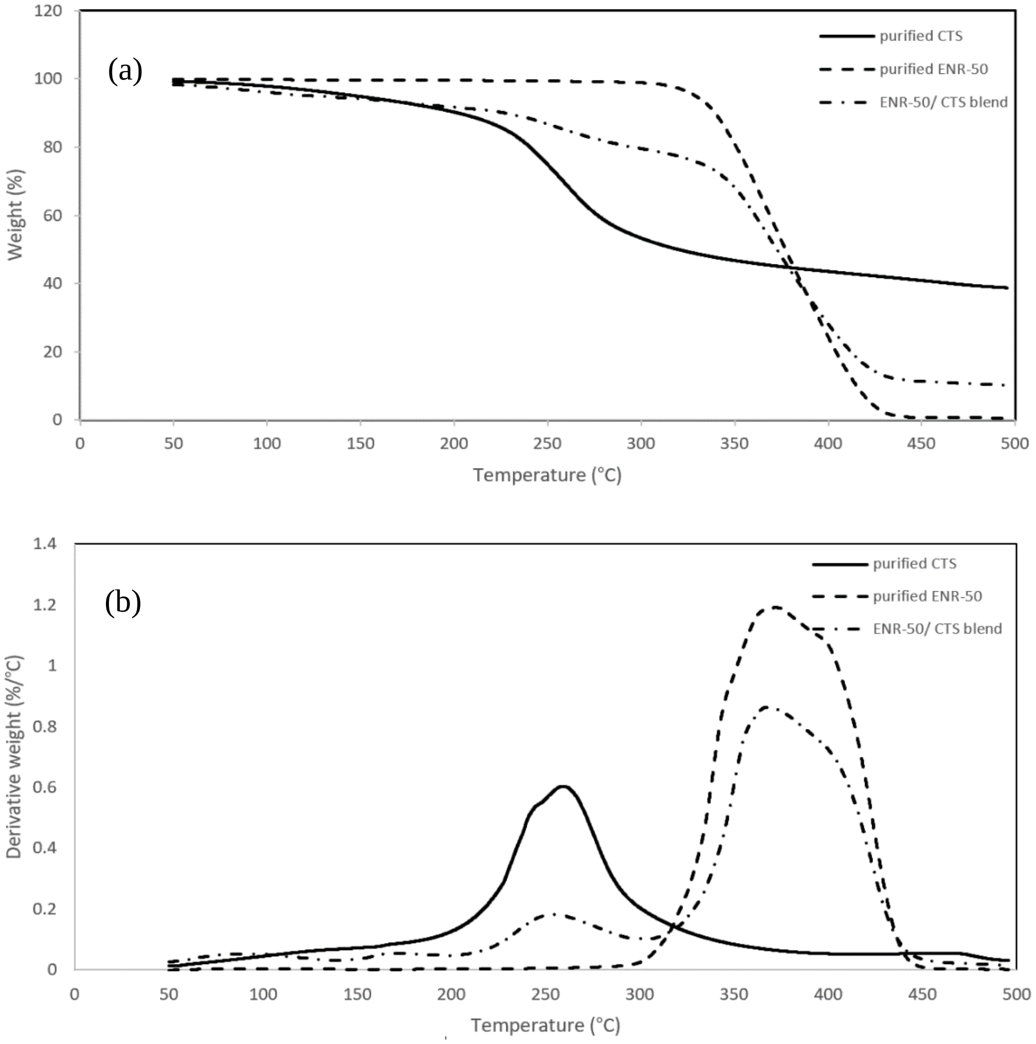

Figure 4. (a) TGA and (b) DTGA curves of the purified CTS, purified ENR-50, and ENR-50/ CTS blend.

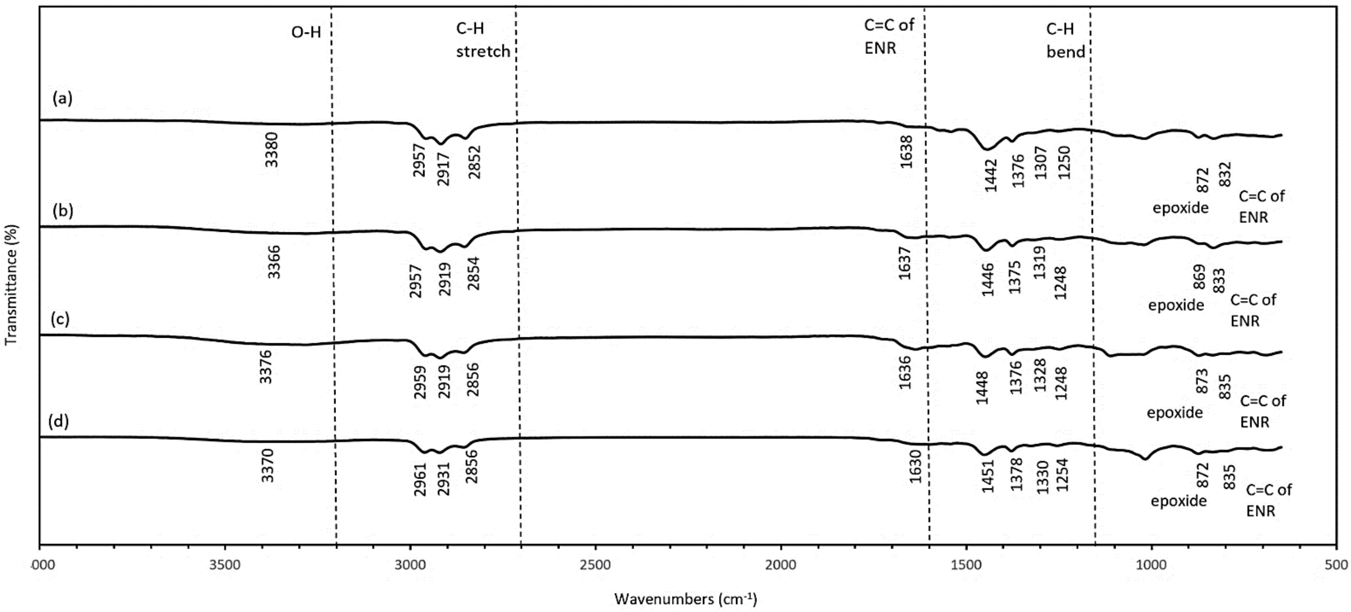

Figure 5. FTIR spectra of (a) unpurified ENR-25, (b) purified ENR-25, (c) unpurified ENR-50, and (d) purified ENR-50.

Fourier Transform Infrared (FTIR)

Figure 5 shows the FTIR spectra of impure and pure samples of both ENR-25 and ENR-50. In this study, the purification step was very important to ensure that the subsequent synthesis and characterization were based on the behaviour of pure samples. During the purification process, an appropriate amount of gel content was removed. If left unremoved, this gel content would later affect the final properties of the blend when the salt was added. This could lead to difficulties in the salt may penetrating the polymer chain due to its high crosslink density [23].

The FTIR spectra of the purified ENR samples showed distinctive peaks related to the hydroxyl group (OH) group and epoxy group (COC). The OH groups in the pure ENR-25 and ENR-50 [Figure 5(b) and (d)] shifted to lower wavenumbers at 3366 cm^{-1} and 3370 cm^{-1}, respectively, compared to the unpurified ENR-25 and ENR-50 [Figure 5(a) and (c)]. This indicates that the OH groups were effectively eliminated, likely by the epoxidation process [22]. The peaks at 2957, 2919, 2854, 1446, 1375, 1319, and 1248 cm^{-1} corresponded to the C-H vibrations of purified ENR-25, while those at 2961, 2931, 2856, 1451, 1378, 1330, and 1254 cm^{-1} corresponded to the C-H vibrations of ENR-50. The peaks at 1637 cm^{-1} and 1630 cm^{-1} belonged to the C=C bonds of ENR-25 and ENR-50, respectively [14, 24]. The COC group shifted to a lower wavenumber at 869 cm^{-1} for purified ENR-25, and 872 cm^{-1} for purified ENR-50, compared to the unpurified samples. This may be due to the successful removal of unreacted epoxy monomers during the purification process [23].

Figure 6 shows the FTIR spectra of the impure and pure CTS samples. The major characteristic peaks of CTS were found around 3384 cm^{-1}, where the OH and NH_2 groups overlapped. Peaks at 3230 cm^{-1} and 3184 cm^{-1} indicated N-H stretching, while peaks at 2933 cm^{-1} and 1452 cm^{-1} corresponded to C-H stretching and C-H bending. A peak at 1552 cm^{-1} belonged to the secondary amide stretching, and peaks at 1078 – 1017 cm^{-1} were characteristic of the C-O stretching vibration. Additionally, a peak at 928 cm^{-1} belonged to the polysaccharide group of chitosan. The purified CTS showed clearer absorption peaks compared to the unpurified CTS. However, the purification of CTS was not really necessary because it had already undergone an isolation process and deacetylation process from chitin. During this process, all minerals, proteins, pigments, and impurities were removed to improve the solubility of CTS [25].

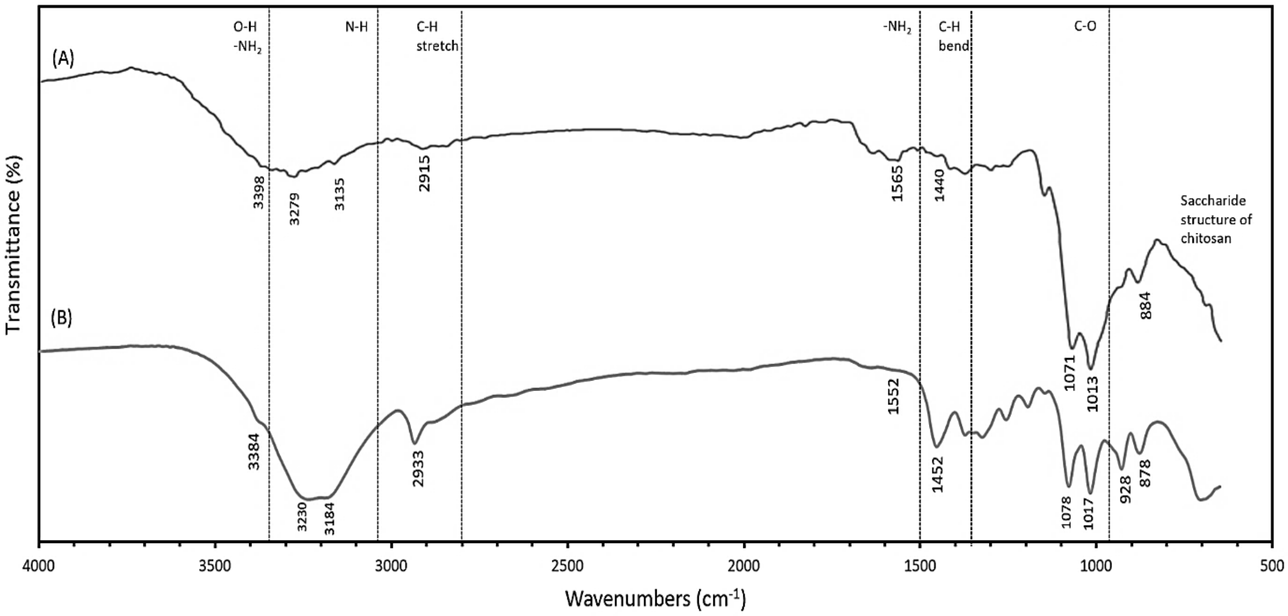

Figure 6. FTIR spectra of (a) unpurified CTS and (b) purified CTS.

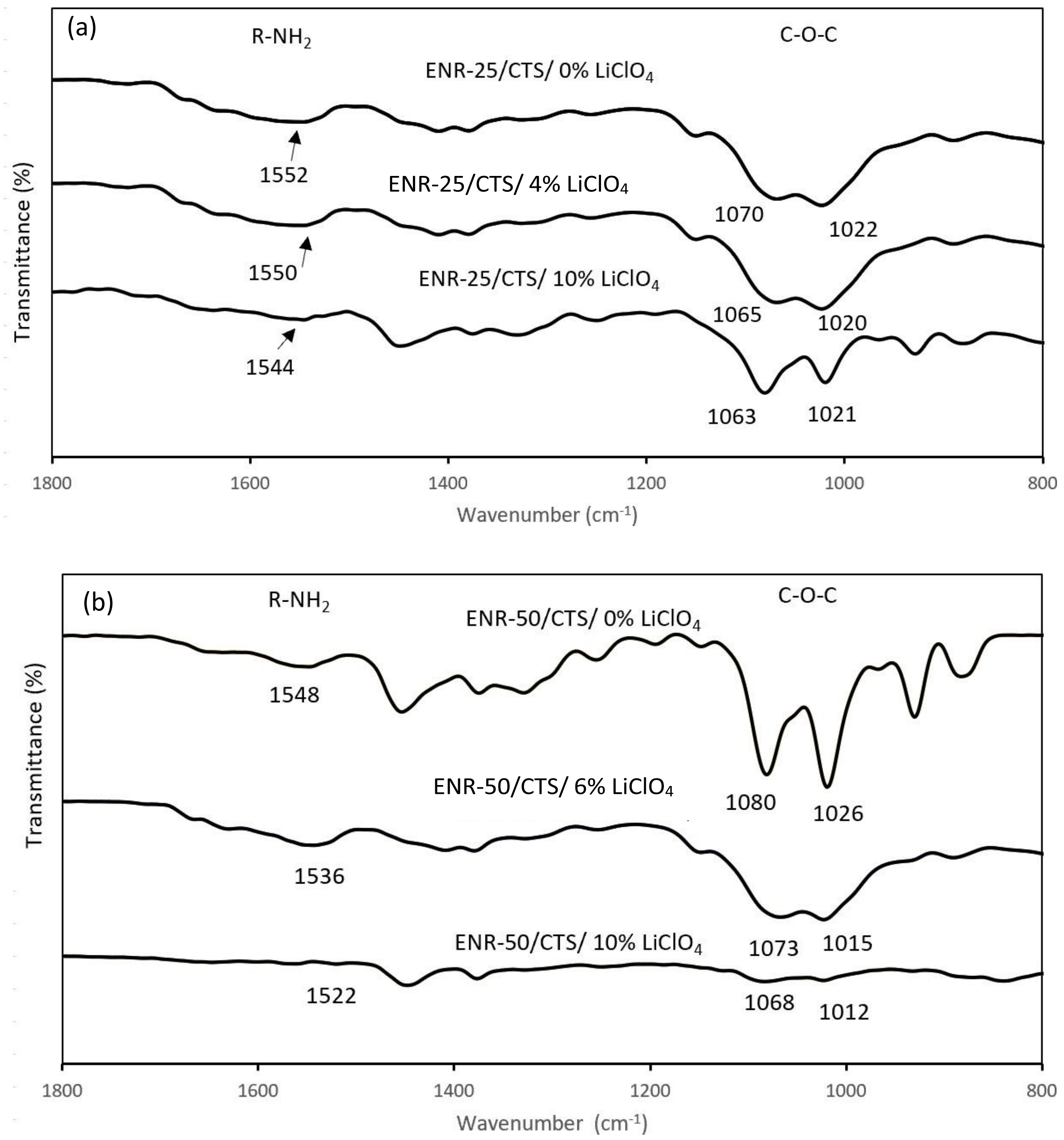

Figure 7. FTIR spectra showing the NH_2 and C-O-C stretching vibrations in (a) ENR-25/CTS/$LiClO_4$, and (b) ENR-50/CTS/$LiClO_4$ at different salt concentrations, in the region of 800 to 1800 cm^{-1}.

Figure 7 shows the FTIR spectra for (a) ENR-25/CTS/$LiClO_4$ and (b) ENR-50/CTS/$LiClO_4$ at different salt concentrations. The fingerprint region of the NH_2 and C-O-C vibrational modes in the ENR and CTS blends was monitored upon doping with $LiClO_4$. In Figure 7(a) and (b), it was observed that the Li^+ cations in the blended system strongly coordinated with the amine group (NH_2) of chitosan, consequently causing a shift in wavenumbers from 1552 to 1544 cm^{-1} and 1548 to 1522 cm^{-1} for the ENR-25 and ENR-50 blend electrolyte systems, respectively. This shift primarily results from the interaction of Li^+ cations with NH_2 [26].

As the $LiClO_4$ concentration increased, the absorption peaks at 1070 and 1022 cm^{-1} shifted to 1063 and 1021 cm^{-1}, respectively, corresponding to the ring stretching of the epoxide group (C- O-C), as shown in Figure 7(a). This was because Li^+ cations coordinated with the epoxide groups as the salt concentration increased [27]. In Figure 7(b), the downshifting of the C-O-C vibrational mode for ENR-50/CTS/$LiClO_4$ was more pronounced compared to ENR-25/CTS/$LiClO_4$, indicating that Li^+ cations coordinated more with the oxygen atom in the epoxide group of the ENR-50/CTS blend than in the ENR-25/CTS blend. The presence of Li^+ ions disrupted the polarity of the oxygen atom in the epoxide group. Therefore, this reduction in intensity of the C-O-C band resulted in the production of ion-dipole interactions.

Electrochemical Impedance Spectroscopy (EIS)

Ionic conductivity (σ) was measured using the AC impedance spectroscopy technique. The bulk resistance, R_b, of the films was determined from the Nyquistplot, where the imaginary part of impedance (Z_i) is plotted against the real part of impedance (Z_r) [28]. Figure 8 shows the conductivity of the blend at different $LiClO_4$ concentrations at ambient temperature. As the salt concentration increased, the conductivity increased reciprocally. This increase is attributed to the greater number of charge carriers due to the high amount of salt dissociation, which simultaneously increases the total ion mobility in the polymer electrolyte system [29]. Furthermore, the segmental motion of ENR and CTS promotes the transport of Li^+ ions to the backbone of the polymer chain. This results in further enhancements in ion mobility and ionic conductivity in the system.

Figure 8 illustrates the variation in wt.% salt concentration of $LiClO_4$ in the ENR-25/CTS blend and the ENR-50/CTS blend. In the blend electrolyte samples, as the wt.% salt concentration increased, the ionic conductivities rose continuously within relatively stable ranges, reaching maximum ion mobility at conductivities of 1.9 x 10^{-3} S/cm for the ENR-25/CTS blend and 2.71 x10^{-3} S/cm for the ENR-50/CTS blend. However, the samples containing 6 wt.% $LiClO_4$ in the ENR-25/CTS blend and 8 wt.% in the ENR-50/CTS blend experienced a drop in ionic conductivity, resulting in reduced ion mobility and a decrease in the number of Li^+ cation charge carriers.

This finding is supported by Battisti & Aroca (1993) [30], who stated that ionic conductivity may decrease as salt concentration increases due to the formation of ion pairs within the polymer chain. As the wt.% salt concentration increased for both blend electrolyte samples, the ionic conductivity values showed a gradual increase, reaching 2.58 x 10^{-3} S/cm for the ENR-25/CTS blend and 3.12 x 10^{-3} S/cm for the ENR-50/CTS blend. The increase in conductivity implied the formation of triple ions within the polymer chain, leading to a gradual increase in conductivity [30], [31]. In addition, the higher conductivity value for ENR-50/CTS/$LiClO_4$ may be attributed to the presence of a higher number of epoxide groups, which act as coordination sites for Li^+ cations [32].

The crosslinking between ENR and the Li^+ cations may result in continuously stable conductivities. To some extent, the separated crosslinking within ENR allows free movement, which could enhance the ionic conductivity of the system [33]. The conductivity values of our polymer blend electrolytes were in agreement with those reported in the literature for similar systems. For example, our ENR-50/CTS/$LiClO_4$ blend exhibited a conductivity of 3.12 x 10^{-3} S/cm, which was higher compared to the 2.58 x 10^{-3} S/cm observed for the ENR-25/CTS/$LiClO_4$ blend. This difference in conductivity can be attributed to the higher number of oxygen atoms present in the epoxide groups of ENR-50, which act as additional coordination sites for Li^+ cations, thereby enhancing ionic conductivity.

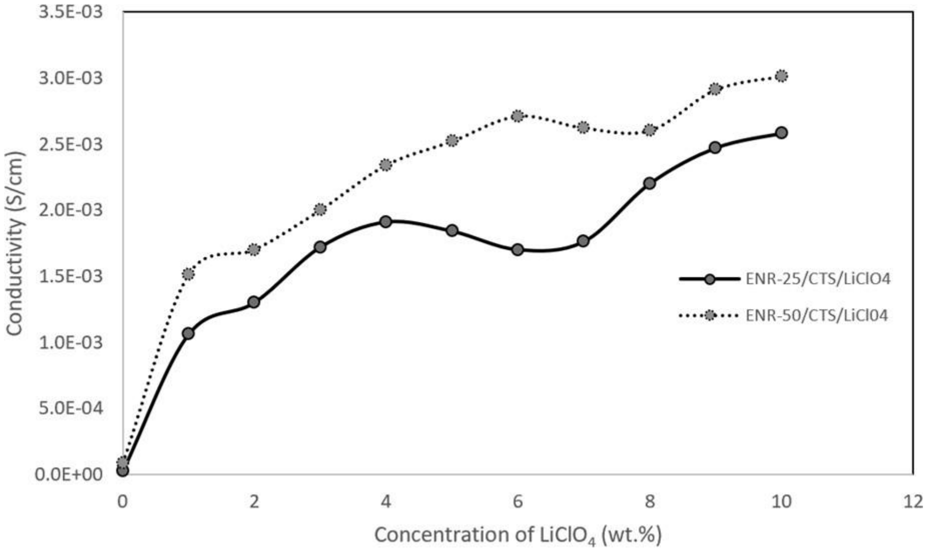

Figure 8. Conductivity against wt.% of $LiClO_4$ in the ENR-25/CTS and ENR-50/CTS blends at ambient temperatures.

CONCLUSION

ENR and CTS were purified using the re-precipitation method and characterized by TGA and ATR-FTIR. The ENR/CTS blend and ENR/CTS/$LiClO_4$ blend electrolyte samples with various concentrations of salt were successfully prepared using the solution casting technique. The effects of $LiClO_4$ in the blended samples were analysed by ATR-FTIR and EIS. The interaction of Li^+ cations with the NH_2 and C-O-C vibrational modes resulted in peak shifting as the salt concentration increased. The conductivity value for ENR- 50/CTS/$LiClO_4$ was 3.12 x 10^{-3} S/cm, which was higher compared to that for ENR-25/CTS/$LiClO_4$, which was 2.58 x 10^{-3} S/cm. This was attributed to the presence of a greater number of oxygen atoms in epoxide groups, which acted as coordination sites for the Li^+ cations.

ACKNOWLEDGEMENTS

This work was supported by the Research Management Centre (RMC) at Universiti Teknologi MARA (UiTM) through the Lestari Grant Scheme (600-RMC/MyRA5/3/LESTARI (011/2020)). The authors would like to thank the Dengkil campus of Universiti Teknologi MARA (UiTM) for providing the facilities. Additionally, the authors express their gratitude to Majlis Amanah Rakyat (MARA) through the Graduate Excellence Programme (GrEP) for providing a scholarship for the completion of this study.

REFERENCES

1. Jinisha, B., KM, A., Manoj, M., Pradeep, P. and Jayalekshmi, J. (2017) Development of a novel type of solid polymer electrolyte for solid state lithium battery applications based on lithium enriched poly (ethylene oxide) (PEO)/poly (vinyl pyrrolidone) (PVP) blend polymer. *Electrochim. Acta*, **235**, 210–222. doi: 10.1016/j.electacta.2017.03.118.

2. Zhang, J., Cao, L. and Chen, Y. (2022) Mechanically robust, self-healing and conductive rubber with dual dynamic interactions of hydrogen bonds and borate ester bonds. *Eur. Polym. J.*, **168**, Apr. 2022. doi: 10.1016/j.eurpolymj.2022.111103.

3. Fonseca, C. P., Rosa, D. S., Gaboardi, F. and Neves, S. (2006) Development of a biodegradable polymer electrolyte for rechargeable batteries. *J. Power Sources*, **155**, 2, 381–384. doi: 10.1016/j.jpowsour.2005.05.004.

4. Juqu, T., Willenberg, S. C., Pokpas, K. and Ross, N. (2022) Advances in paper-based battery research for biodegradable energy storage. *Advanced Sensor and Energy Materials*, **1**, 4, 100037. doi: 10.1016/j.asems.2022.100037.

5. Jantanasakulwong, K., Leksawasdi, N. and Seesuriyachan, P. (2016) Reactive blending of thermoplastic starch, epoxidized natural rubber and chitosan. *Eur. Polym. J.*, **84**, 292–299. doi: 10.1016/j.eurpolymj.2016.09.035.

6. Abu Bakar, M., Ismail, J., Teoh, C. H., Tan, W. L. and Abu Bakar, N. H. H. (2008) Modified natural rubber induced aqueous to toluene phase transfer of gold and platinum colloids. *J. Nanomater*, **2008**, 1. doi: 10.1155/2008/130295.

7. Rooshenass, P., Yahya, R. and Gan, S. N. (2016) Comparison of three different degradation methods to produce liquid epoxidized natural rubber. *Rubber Chemistry and Technology*, **89**, 1, 177–198, Mar. 2016. doi: 10.5254/RCT.15.84878.

8. Desai, N., *et al.* (2023) Chitosan: A Potential Biopolymer in Drug Delivery and Biomedical Applications. *MDPI*, Apr. 01, 2023. doi: 10.3390/pharmaceutics15041313.

9. Chen, Q., *et al.* (2022) Progress in Research of Chitosan Chemical Modification Technologies and Their Applications. *MDPI*, Aug. 01, 2022. doi: 10.3390/md20080536.

10. Mohamed, S. N., Johari, N. A., Ali, A. M. M., Harun, M. K. and Yahya, M. Z. A. (2008) Electrochemical studies on epoxidised natural rubber-based gel polymer electrolytes for lithium-air cells. *J. Power Sources*, **183**, 1, 351–354, Aug. 2008. doi: 10.1016/j.jpowsour.2008.04.048.

11. Satchanska, G., Davidova, S. and Petrov, P. D. (2024) Natural and Synthetic Polymers for Biomedical and Environmental Applications. *Multidisciplinary Digital Publishing Institute (MDPI)*, Apr. 01, 2024. doi: 10.3390/polym16081159.

12. Ilyas, R. A., *et al.* (2022) Natural-Fiber-Reinforced Chitosan, Chitosan Blends and Their Nanocomposites for Various Advanced Applications. *MDPI*, Mar. 01, 2022. doi: 10.3390/polym14050874.

13. Taweepreda, W. and Wichianchom, A. (2014) Fabrication and characterization of epoxidized natural rubber-chitosan membrane. In *Advanced Materials Research*, 205–208. doi: 10.4028/www.scientific.net/AMR.844.205.

14. Dahham, O. S., *et al.* (2018) Studies of ENR-25/TiO2 Composites for Electronic Materials Packaging Applications. In *Journal of Physics: Conference Series, Institute of Physics Publishing*, Jun. 2018. doi: 10.1088/1742-6596/1019/1/012054.

15. Aziz, S. B., Woo, T. J., Kadir, M. F. Z. and Ahmed, H. M. (2018) A conceptual review on

polymer electrolytes and ion transport models. *Elsevier B.V.*, Mar. 01, 2018. doi: 10.1016/j.jsamd.2018.01.002.

16. Mahmood, L. I., *et al.* (2018) Li+ doped chitosan-based solid polymer electrolyte incorporated with PEDOT:PSS for electrochromic device. *Journal of the Turkish Chemical Society, Section A: Chemistry*, **5**, 3, 1413–1422. doi: 10.18596/jotcsa.433901.

17. Obino, V. and Yadav, U. (2021) Application of Polymer Based Nanocomposites for Water Shutoff—A Review. *Fuels*, **2**, 3, 304–322. doi: 10.3390/fuels2030018.

18. Rayung, M., *et al.* (2020) Bio-based polymer electrolytes for electrochemical devices: Insight into the ionic conductivity performance. *Materials*, **13**, 4. doi: 10.3390/ma13040838.

19. Vincent, C. A., *et al.* (2020) A Biodegradable Secondary Battery and its Biodegradation Mechanism for Eco-Friendly Energy-Storage Systems. *Polymer Bulletin*, **7**, 4, 1–10. doi: 10.1002/adma.202004902.

20. Harun, F. and Chan, C. H. (2017) Electronic Applications of Polymer Electrolytes of Epoxidized Natural Rubber. December, 2017. doi: 10.1007/978-3-319-23663-6.

21. Aranaz, I., Alc, R. and Concepci, M. (2021) Chitosan: An Overview of Its Properties and Applications.

22. Phinyocheep, P. (2014) Chemical modification of natural rubber (NR) for improved performance. In *Chemistry, Manufacture and Applications of Natural Rubber*, *Elsevier Inc.*, 68–118. doi: 10.1533/9780857096913.1.68.

23. Yong, M. Y., Ang, D. T. C. and Sarih, N. M. (2019) Novel natural rubber-based epoxy coating. *Prog. Org. Coat*, **135**, 105–113, Oct. 2019. doi: 10.1016/j.porgcoat.2019.05.040.

24. Algaily, B., Kaewsakul, W., Sarkawi, S. S. and Kalkornsurapranee, E. (2021) Enabling reprocessability of ENR-based vulcanisates by thermochemically exchangeable ester crosslinks. *Plastics, Rubber and Composites*, **50**, 7, 315–328. doi: 10.1080/14658011.2021.1896093.

25. Pellis, A., Guebitz, G. M. and Nyanhongo, G. S. (2022) Chitosan: Sources, Processing and Modification Techniques. *Gels*, **8**, 7, Jul. 2022. doi: 10.3390/gels8070393.

26. Li, O., Li, S., Younesi, R., Veith, G. M., Johansson, P. and Edstro, D. K. (2015) Environmental Science Lithium salts for advanced lithium batteries. **Il**, 1905–1922. doi: 10.1039/c5ee01215e.

27. Singh, T. H. J. and Bhat, S. V. (2003) Morphology and conductivity studies of a new solid polymer. **26**, 7, 707–714.

28. Norjeli, M. F., Tamchek, N., Osman, Z., Mohd Noor, I. S., Kufian, M. Z. and Ghazali, M. I. B. M. (2022) Additive Manufacturing Polyurethane Acrylate via Stereolithography for 3D Structure Polymer Electrolyte Application. *Gels*, **8**, 9, Sep. 2022. doi: 10.3390/gels8090589.

29. Li, Q., Chen, J., Fan, L., Kong, X. and Lu, Y. (2016) Progress in electrolytes for rechargeable Li-based batteries and beyond. *Green Energy and Environment*, **1**, 1, 18–42. doi: 10.1016/j.gee.2016.04.006.

30. Battisti, D. and Aroca’, R. (1993) Vibrational Studies of Lithium Perchlorate in Propylene Carbonate Solutions.

31. Tominaga, Y. (2017) Ion-conductive polymer electrolytes based on poly(ethylene carbonate) and its derivatives. *Nature Publishing Group*, Mar. 01, 2017. doi: 10.1038/pj.2016.115.

32. Mohd Yusoff, S. N. H., Sim, L. H., Chan, C. H., Sheikh Abdul Aziz, S. S., Mahmud, Z. S. and Mohd Hairi, H. (2015) Studies on Thermal and Conductivity of Modified Natural Rubber.

33. Zainal, N., Mohamed, N. S., Idris R., Z. N., M. N. S., and I. R. (2013) Properties of ENR -50 Based Electrolyte System. **42**, 4, 481–485.